Available online at www.sciencedirect.com
SCIENCE DIRECT®
Journal of Nuclear Materials 340 (2005) 39–51
journal of nuclear materials
www.elsevier.com/locate/jnucmat

Chlorination of UO_2, PuO_2 and rare earth oxides using $ZrCl_4$ in LiCl–KCl eutectic melt

Yoshiharu Sakamura [a,*], Tadashi Inoue [a], Takashi Iwai [b], Hirotake Moriyama [c]

[a] Central Research Institute of Electric Power Industry (CRIEPI), Iwadokita 2-11-1, Komae-shi, Tokyo 201-8511, Japan
[b] Japan Atomic Energy Research Institute (JAERI), Oarai-machi, Higashiibaraki-gun, Ibaraki-ken 311-1394, Japan
[c] Department of Nuclear Engineering, Kyoto University, Yoshidahonmachi, Sakyo-ku, Kyoto 606-8501, Japan

Received 12 April 2004; accepted 5 November 2004

Abstract

A new chlorination method using $ZrCl_4$ in a molten salt bath has been investigated for the pyrometallurgical reprocessing of nuclear fuels. $ZrCl_4$ has a high reactivity with oxygen but is not corrosive to refractory metals such as steel. Rare earth oxides (La_2O_3, CeO_2, Nd_2O_3 and Y_2O_3) and actinide oxides (UO_2 and PuO_2) were allowed to react with $ZrCl_4$ in a LiCl–KCl eutectic salt at 773 K to give a metal chloride solution and a precipitate of ZrO_2. An addition of zirconium metal as a reductant was effective in chlorinating the dioxides. When the oxides were in powder form, the reaction was observed to progress rapidly. Cyclic voltammetry provided a convenient way of establishing when the reaction was completed. It was demonstrated that the $ZrCl_4$ chlorination method, free from corrosive gas, was very simple and useful.

PACS: 28.41.Bm; 82.40.−g

1. Introduction

The next generation nuclear fuel cycle must not only deliver economic advantages but must also be environmentally safe and highly resistant to nuclear proliferation. Combining the metal fuel fast reactor with excellent safety features and pyrometallurgical reprocessing that provides simple and compact facilities is one of the promising options [1–3].

In pyrometallurgical reprocessing, uranium, plutonium and minor actinides are recovered by the electrorefining process shown in Fig. 1. The actinides in the chopped spent metal fuels (i.e. irradiated U–Zr or U–Pu–Zr) are anodically dissolved into a LiCl–KCl eutectic electrolyte at 773 K [4,5]. At the same time, highly pure uranium is collected onto the solid cathode [6,7]. A mixture of plutonium, uranium and minor actinides is collected by employing a liquid cadmium cathode [5,8–10]. Active fission products such as cesium, strontium and rare earths accumulate in the electrolyte salt, while noble fission products such as molybdenum, palladium and ruthenium do not dissolve and remain at the anode.

The cathode products are distilled in the cathode processor at a high temperature to remove the adhering salt electrolyte and cadmium from the actinide metals [11].

* Corresponding author. Tel.: +81 3 3480 2111; fax: +81 3 3480 7956.
E-mail address: sakamura@criepi.denken.or.jp (Y. Sakamura).

0022-3115/$ - see front matter © 2004 Elsevier B.V. All rights reserved.
doi:10.1016/j.jnucmat.2004.11.002

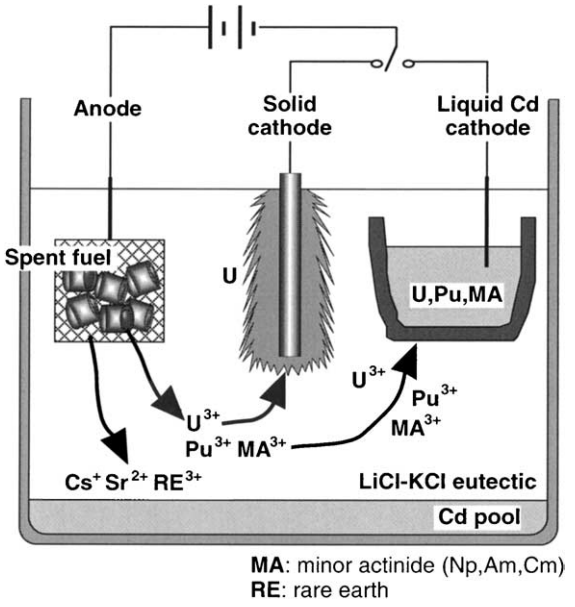

Fig. 1. Schematic of the electrorefining process for metal fuel reprocessing.

Then, the metal fuel slugs are made by injection casting using the recovered actinides and metallic zirconium [12,13]. In these two processes, a carbon crucible coated with ZrO_2 or Y_2O_3 is used to contain the corrosive materials.

When the electrorefining process is applied to oxide nuclear fuels, the oxides have to be treated to remove oxygen. Therefore, a lithium reduction process to reduce oxides into metal form in a molten LiCl bath [14–16] and a chlorination process using chlorine gas [17] have been developed. In these processes, corrosive materials such as metallic lithium, Li_2O and Cl_2 are handled at a high temperature of 923–973 K and a salt bath different from the LiCl–KCl eutectic is employed, which may make the design of a pyrometallurgical reprocessing facility more challenging.

We propose a new chlorination method using $ZrCl_4$ instead of Cl_2 to convert oxides and oxychlorides into chlorides. $ZrCl_4$ has a high reactivity with oxygen, but is not corrosive to refractory metals such as iron and nickel. The actinide and rare earth oxides are allowed to react with $ZrCl_4$ in a molten salt bath to give metal chlorides dissolved in the salt and a precipitate of ZrO_2. This simple chlorination method is quite compatible with the electrorefining process because zirconium is a major component of the metal fuels and LiCl–KCl eutectic at 773 K is used as the salt bath. The actinides dissolved in the salt can be collected in the same manner as indicated in Fig. 1.

In this paper, 'rare earth elements' indicate yttrium and lanthanide elements of which atomic number is not more than 64 (i.e. from lanthanum to gadolinium).

2. Thermodynamic estimation

$ZrCl_4$ has a high reactivity with oxygen and donates a chloride ion as indicated by the following equation:

$$ZrCl_4 + 2\,O^{2-} \rightarrow ZrO_2 + 4\,Cl^- \quad (1)$$

The standard Gibbs free energy changes (ΔG°) in reactions expected for the $ZrCl_4$ chlorination process were calculated by using a thermodynamic database [18]. Table 1 shows ΔG° (kcal/mol of oxygen) of actinides and rare earth fission products obtained with the oxides, chlorides, oxychlorides and metals in their standard states at 773 K. Uranium, neptunium and plutonium in the trivalent state are stable in the LiCl–KCl eutectic system, while the starting materials are dioxides. Therefore, in order to reduce the actinides from a tetravalent to a trivalent state, zirconium metal is used as a reductant in the reactions (T1), (T5) and (T8). In practice, a small amount of Zr(II) that denotes divalent zirconium in the salt phase is conveniently yielded in the salt by the following reaction in the presence of zirconium metal [19]:

Table 1
ΔG° for reactions of actinide and rare-earth oxides with $ZrCl_4$ at 773 K

	Reaction	ΔG° (kcal/mol-O)
U:		
(T1)	$UO_2 + 3/4\,ZrCl_4 + 1/4\,Zr \rightarrow UCl_3 + ZrO_2$	−13.5
(T2)	$UO_2 + ZrCl_4 \rightarrow UCl_4 + ZrO_2$	−1.9
(T3)	$UO_2 + 1/2\,ZrCl_4 \rightarrow UOCl_2 + 1/2\,ZrO_2$	−2.9
(T4)	$UOCl + 1/2\,ZrCl_4 \rightarrow UCl_3 + 1/2\,ZrO_2$	−16.7
Np:		
(T5)	$NpO_2 + 3/4\,ZrCl_4 + 1/4\,Zr \rightarrow NpCl_3 + ZrO_2$	−24.1
(T6)	$NpO_2 + ZrCl_4 \rightarrow NpCl_4 + ZrO_2$	−4.4
(T7)	$NpO_2 + 1/2\,ZrCl_4 \rightarrow NpOCl_2 + 1/2\,ZrO_2$	−4.8
Pu:		
(T8)	$PuO_2 + 3/4\,ZrCl_4 + 1/4\,Zr \rightarrow PuCl_3 + ZrO_2$	−29.4
(T9)	$PuOCl + 1/2\,ZrCl_4 \rightarrow PuCl_3 + 1/2\,ZrO_2$	−16.2
(T10)	$Pu_2O_3 + 3/2\,ZrCl_4 \rightarrow 2\,PuCl_3 + 3/2\,ZrO_2$	−29.5
Y:		
(T11)	$Y_2O_3 + 3/2\,ZrCl_4 \rightarrow 2\,YCl_3 + 3/2\,ZrO_2$	−17.0
La:		
(T12)	$La_2O_3 + 3/2\,ZrCl_4 \rightarrow 2\,LaCl_3 + 3/2\,ZrO_2$	−35.7
(T13)	$LaOCl + 1/2\,ZrCl_4 \rightarrow LaCl_3 + 1/2\,ZrO_2$	−23.4
Ce:		
(T14)	$CeO_2 + 3/4\,ZrCl_4 + 1/4\,Zr \rightarrow CeCl_3 + ZrO_2$	−36.3
(T15)	$CeO_2 + ZrCl_4 \rightarrow CeCl_3 + ZrO_2 + 1/2\,Cl_2$	−13.0
(T16)	$Ce_2O_3 + 3/2\,ZrCl_4 \rightarrow 2\,CeCl_3 + 3/2\,ZrO_2$	−33.4
Nd:		
(T17)	$Nd_2O_3 + 3/2\,ZrCl_4 \rightarrow 2\,NdCl_3 + 3/2\,ZrO_2$	−28.6
(T18)	$NdOCl + 1/2\,ZrCl_4 \rightarrow NdCl_3 + 1/2\,ZrO_2$	−17.8

$$Zr(IV) + Zr \rightarrow 2\,Zr(II) \quad (2)$$

Zr(II) is expected to serve as a reductant species, which may accelerate the chlorination. If no reductant is present in the chlorination system for UO_2 and NpO_2, tetravalent chloride or oxychloride will be supplied. As for plutonium, PuOCl is known to be stable and will also be chlorinated with $ZrCl_4$. It can be seen from Table 1 that uranium is the most difficult actinide to chlorinate among the three actinides.

The rare earth group amounts to about 30 wt% of fission product and is chemically similar to the actinides. According to Table 1, the rare earth oxides and oxychlorides can be converted into chlorides by using $ZrCl_4$. ΔG° in the following reaction for the rare earth sesquioxide was plotted against the radius of trivalent ion [20]:

$$RE_2O_3 + 3/2\,ZrCl_4 \rightarrow 2\,RECl_3 + 3/2\,ZrO_2 \quad (3)$$

where RE denotes a rare earth. It is obvious from Fig. 2 that ΔG° increases with decreasing ionic radius and that yttrium is the most difficult element to chlorinate among the rare earths examined.

In general, chemical characteristics of the transplutonium elements such as americium and curium are between those of plutonium and the rare earth group. Hence, if the chlorination of plutonium and rare earth oxides succeeds, the transplutonium oxides will also be chlorinated.

Thermodynamic considerations suggest that all the actinide and rare earth oxides related to the spent nuclear fuel will be converted into chloride using $ZrCl_4$. However, it is necessary to verify the reactions in the actual systems by performing experiments. Because a LiCl–KCl eutectic salt bath is used in the $ZrCl_4$ chlorination process to facilitate handling, the activity coefficients of the metal chlorides in the salt may influence which reaction occurs in the system. The activity coefficient of $ZrCl_4$ in the salt is known to be very small since chloride ions coordinate to give stable hexachlorocomplex, $ZrCl_6^{2-}$ [21]. Most actinide and rare earth ions also exist in the salt as the octahedral complex anion. Moreover, the reaction rate is very important to judge whether the chlorination process is of practical use. The morphology of the by-product, ZrO_2, has to be investigated to determine the practicality of separating the ZrO_2 from the molten salt.

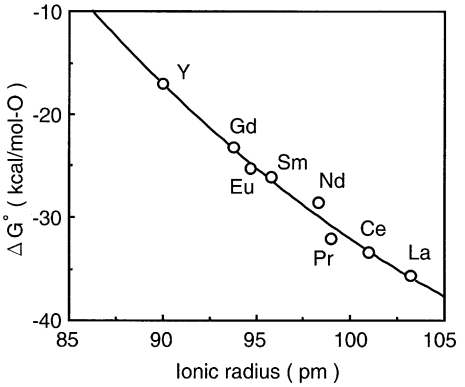

Fig. 2. The relationships between ΔG° for the following reaction and ionic radius of rare earth:

$$RE_2O_3 + (3/2)ZrCl_4 \rightarrow 2\,ECl_3 + (3/2)ZrO_2$$

3. Experimental

3.1. Materials and equipment

High purity LiCl–KCl eutectic (59:41 mole ratio), $ZrCl_4$ with a purity of 99.9% and LiCl–KCl eutectic containing 1 wt% of AgCl were obtained from Anderson Physics Laboratory. To avoid vaporization of $ZrCl_4$, which sublimes above 573 K, LiCl–KCl–$ZrCl_4$ mixtures were prepared by heating a sealed quartz tube containing LiCl–KCl eutectic and $ZrCl_4$ up to 823 K. Once $ZrCl_4$ dissolved into a molten LiCl–KCl eutectic, $ZrCl_4$ did not escape as vapor from the salt [19]. Rare earth oxides (La_2O_3, CeO_2 and Nd_2O_3) of >99.5% purity were purchased from Wako Pure Chemical Industries, Ltd. Zirconium wire (99.5% purity), molybdenum wire (99.95% purity), tantalum wire (99.95% purity) and silver wire (99.99% purity) were supplied by Rare Metallic Co., Ltd.

All of the experiments using molten salts were conducted in a high-purity argon atmosphere glove box in which the concentrations of oxygen and moisture were controlled to be less than 2 ppm. A model 273A potentiostat/galvanostat of EG&G Princeton Applied Research and an EG&G M270 computer software were used for the cyclic voltammetry study.

Salt samples taken from molten salts were dissolved in water and filtrated using 0.45 μm MILLIPORE filter, when chlorides dissolved into the water were separated from any oxide and oxychloride precipitates. Then, actinide, rare earth and zirconium concentrations in the filtrate were determined by an inductively coupled plasma atomic emission spectrometer (ICP-AES), IRIS Advantage of Jarrell Ash. The precipitates remaining on the filter were identified by an X-ray diffraction (XRD) technique using a RINT 2500 V of Rigaku and by WDX/EDX EPMA using a JXA-8900RL of JEOL.

3.2. $ZrCl_4$ solubility measurements

Solubility of $ZrCl_4$ in the LiCl–KCl eutectic was measured since it may affect the chlorination rate. Four test samples were prepared by sealing a quartz tube containing about 0.1 g of LiCl–KCl eutectic and a given weight of $ZrCl_4$. The experimental apparatus is shown schematically in Fig. 3. The samples were heated slowly in a

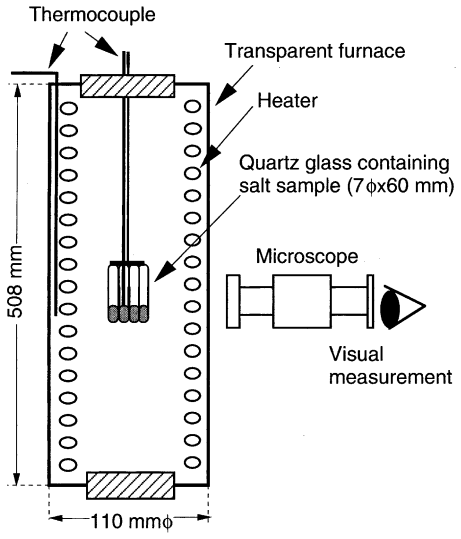

Fig. 3. Experimental apparatus for measuring the $ZrCl_4$ solubility in LiCl–KCl eutectic.

transparent furnace (Gold Furnace, TRANS-TEMP Co.). After the bulk salt melted at 625 K, some crystals like granulated sugar or needles were seen at the bottom of the quartz tube. Then, the temperature at which the precipitate completely disappeared was determined by microscopic observation. The measurement was repeated several times and the precision of the liquidus temperature was estimated to be ±1 K. The crystal like granulated sugar formed when the test sample was cooled slowly. After the measurements, the $ZrCl_4$ contents of the test samples were determined by ICP-AES analysis.

3.3. Chlorination tests for rare earth oxides

The chlorination experiments using La_2O_3, Nd_2O_3, Y_2O_3 and CeO_2 were carried out. In the La_2O_3 test, the products were examined by varying both the amount of $ZrCl_4$ added and the reaction time. In the Nd_2O_3 test, the behavior of neodymium and zirconium was investigated by cyclic voltammetry during chlorination. A chlorination test using a sintered Y_2O_3 was attempted since a dense Y_2O_3 chip is generally the most difficult rare earth oxide sample to chlorinate. CeO_2, a surrogate of actinide dioxides, was chlorinated both in the presence and in the absence of a reductant of zirconium metal.

3.3.1. La_2O_3

Weighted amounts of La_2O_3 in powder form, LiCl–KCl eutectic, LiCl–KCl–$ZrCl_4$ (29.4wt%$ZrCl_4$) were loaded into a Pyrex test tube. Table 2 shows the experimental conditions. An excess amount of $ZrCl_4$ relative to the amount of La_2O_3 was loaded in Run La-1 and La-2, while half that amount of $ZrCl_4$ was loaded in Run La-3 and La-4. The four Pyrex test tubes were put into an electric furnace and the temperature was maintained at 773 K. The molten salt was mixed with a tantalum wire at intervals. After 8 or 73 h, the test tubes were taken out from the furnace for sudden cooling. Each sample was dissolved in water, followed by filtration for the analyses. It took a long time to filtrate the solution using 0.45 μm filter for Run La-1 and La-2.

3.3.2. Nd_2O_3

Nd_2O_3 powder (0.224 g) and LiCl–KCl eutectic (43.6 g) were contained in an alumina crucible at 773 K. Electrodes, a tantalum stirrer and a thermocouple were placed in the melt as shown in Fig. 4. The working electrode was a molybdenum wire, 1 mm in diameter, which had an alumina tube insulator for determining the surface area. An 8 mm portion of the electrode wire was exposed to the electrolyte. A molybdenum wire with a spiral at its lower end was employed as the counter electrode. The reference electrode was an Ag/AgCl electrode consisting of a silver wire immersed in the LiCl–KCl eutectic mixture with 1wt%AgCl, which was contained in a closed-end Pyrex tube.

An addition of LiCl–KCl–29.4wt%$ZrCl_4$ mixture was carried out five times (0.307 g, 0.302 g, 0.311 g, 0.098 g and 0.103 g). After each addition, the reaction was allowed to proceed and then cyclic voltammograms were measured, followed by taking salt samples to allow analysis of the concentration of neodymium and zirconium.

3.3.3. Y_2O_3

A dense Y_2O_3 crucible ($5\varnothing \times 5$ mmH, 0.212 g, >99.5% purity) provided by TEP Ltd. was used as the oxide sample. The Y_2O_3 crucible was put in the LiCl–KCl eutectic melt (10.1 g) contained in an alumina crucible at 773 K. Then, LiCl–KCl–34.2wt%$ZrCl_4$ mixture (1.01 g) was added, followed by the taking of salt samples at intervals. After 98 h, the Y_2O_3 crucible was pulled out from the melt for observation. The crucible became thin and was easily crushed by pressing with a quartz rod.

3.3.4. CeO_2

Two alumina crucibles containing a weighed amount of CeO_2 in powder form and LiCl–KCl eutectic were maintained at 773 K. A stirrer made of zirconium metal wire was placed in the crucible for Run Ce-1. A quartz rod was used for stirring in Run Ce-2. Then, about 0.7 g of LiCl–KCl–34.2wt%$ZrCl_4$ mixture was added three times into each crucible. The amounts of the salt and oxide used in the tests are shown in Table 3. After each addition, the two melts were stirred. Then, salt samples were taken at intervals to investigate the time dependence of the metal chloride concentration in the salt phase.

Table 2
Experimental conditions and analytical results of the product of the La_2O_3 chlorination tests

Run no.	Oxide and salt loaded (g)			Reaction time at 773 K (h)	Metal in the salt phase after the reaction (g)		Precipitate[a]
	La_2O_3	LiCl–KCl–$ZrCl_4$ (29.4wt%$ZrCl_4$)	LiCl–KCl eutectic		La	Zr	
La-1	0.196	0.804	7.196	8	0.137	0.0063	ZrO_2
La-2	0.205	0.814	7.187	73	0.143	0.0028	ZrO_2
La-3	0.199	0.396	7.605	8	0.067	ND[b]	LaOCl + α[c]
La-4	0.199	0.397	7.609	73	0.070	ND	LaOCl + α

[a] Identified by XRD.
[b] Not detected by ICP-AES.
[c] Un-assigned peaks that might be attributable to a La–Zr complex oxide.

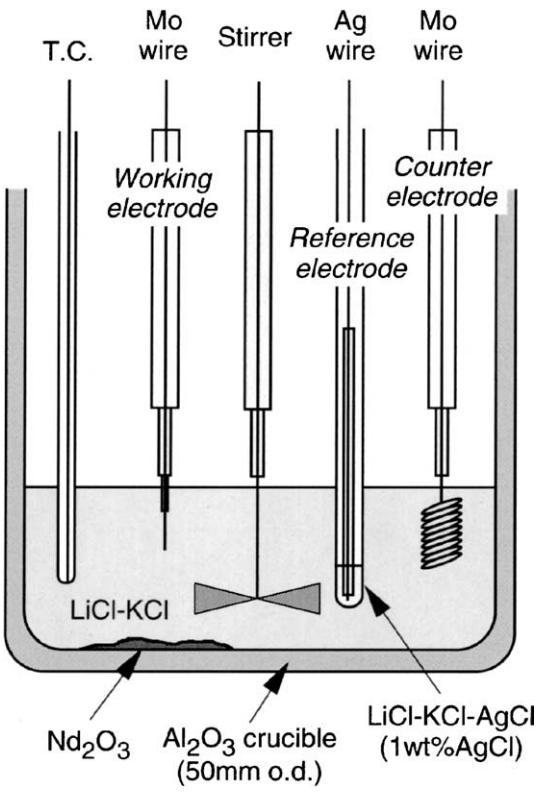

Fig. 4. Electrochemical cell for the Nd_2O_3 chlorination test.

3.4. Chlorination tests for actinide oxides

The chlorination experiments using UO_2 and PuO_2 were carried out.

3.4.1. UO_2

The chlorination tests for UO_2 were carried out both in the presence and in the absence of a zirconium metal reductant. In Run U-1, an alumina crucible containing LiCl–KCl eutectic, LiCl–KCl–29.4wt%$ZrCl_4$ mixture and UO_2 was heated up to 773 K. The amounts of the salts and oxide are shown in Table 4. The molten salt was stirred with a zirconium metal rod. The salt became dark wine red, which indicated that trivalent uranium existed in the salt. After a salt sample was taken, an excess amount of LiCl–KCl–29.4wt%$ZrCl_4$ mixture was added into the salt for the complete chlorination.

In Run U-2, a Pyrex test tube containing LiCl–KCl eutectic, LiCl–KCl–5.6wt%$ZrCl_4$ mixture and UO_2 was heated up to 773 K. The molten salt was stirred with a quartz rod. The salt became yellow green, which indicated that tetravalent uranium existed in the salt. After 4 h, a salt sample was taken, as long as a precipitate of UO_2 remained. A Pyrex container is a convenient means of observing the molten salt, but it was colored black when zirconium metal was present in the system. This may have been due to corrosion from Zr(II) produced by the reaction (2).

3.4.2. PuO_2

The chlorination test for PuO_2 was carried out in the presence of a zirconium metal reductant. An alumina crucible containing LiCl–KCl eutectic (22.966 g), LiCl–KCl–6.2wt%$ZrCl_4$ mixture (1.895 g) and PuO_2 (0.101 g) was heated up to 773 K. The molten salt bath was stirred with a zirconium metal rod and salt samples were taken at intervals. The salt became blue, which indicated that trivalent plutonium existed in the salt.

4. Results and discussion

4.1. $ZrCl_4$ solubility measurements

The liquidus temperature of each salt sample sealed in the quartz tube was visually determined and is shown in Table 5. As shown in Fig. 5, the logarithm of the solubility vs. the reciprocal temperature gives an

Table 3
Experimental conditions for the CeO_2 chlorination test

Run no.	Oxide and salt loaded (g)		LiCl–KCl–34.2wt%$ZrCl_4$ added (g)			Reductant
	CeO_2	LiCl–KCl	First	Second	Third	Zr metal
Ce-1	0.490	20.000	0.718	0.751	0.714	Used
Ce-2	0.494	20.002	0.718	0.753	0.720	Not used

Table 4
Experimental conditions for the UO_2 chlorination test

Run no.	Oxide and salt loaded (g)			Salt added (g)	Reductant
	UO_2	LiCl–KCl	LiCl–KCl–$ZrCl_4$	LiCl–KCl–$ZrCl_4$	Zr metal
U-1	0.099	8.505	0.150[a]	1.003[a]	Used
U-2	0.190	8.492	2.822[b]	–	Not used

[a] $ZrCl_4$ content: 29.4 wt%.
[b] $ZrCl_4$ content: 5.6 wt%.

Table 5
Results of the $ZrCl_4$ solubility measurement

Sample no.	Liquidus temperature (K)	$ZrCl_4$ content[a] (wt%)
#1	761	4.31
#2	707	2.25
#3	668	1.08
#4	637	0.533

[a] Determined by ICP-AES analysis.

approximately linear relationship and is represented by the equation:

$$\log X_{ZrCl_4} = 2.793 - 3606/T, \quad (4)$$

where X_{ZrCl_4} is mole fraction of $ZrCl_4$ in LiCl–KCl eutectic and T is K. The solubility at 773 K is computed to be not less than 1.3 at.%. It has been reported that $ZrCl_4$ reacts with ACl to give A_2ZrCl_6, where A denotes an alkali metal cation, and that the thermodynamic stability of A_2ZrCl_6 increases as the size of A increases from lithium to cesium [22]. Therefore, the compound precipitating in the LiCl–KCl eutectic system by add-ing an excess of $ZrCl_4$ is probably K_2ZrCl_6. The XRD pattern measured for the prepared LiCl–KCl–29.4wt%$ZrCl_4$ at room temperature indicated that the salt sample consisted of LiCl–KCl eutectic and K_2ZrCl_6.

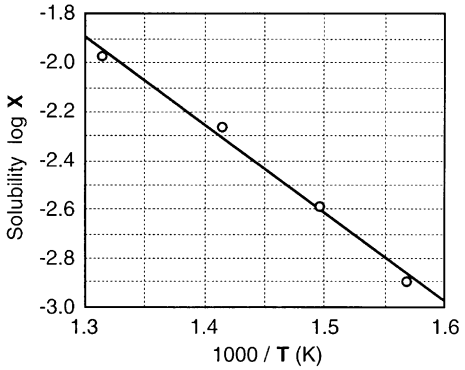

Fig. 5. Solubility of $ZrCl_4$ in LiCl–KCl eutectic.

4.2. Chlorination of rare earth oxides

4.2.1. La_2O_3

The results of the La_2O_3 chlorination test are shown in Table 2. When an excess amount of $ZrCl_4$ was loaded in Run La-1 and La-2, all of the lanthanum dissolved and some $ZrCl_4$ remained in the salt. The micrograph for the precipitate of Run La-2 in Fig. 6(a) shows that the particle size was less than about 100 μm, and the EPMA analysis demonstrated that there was no lanthanum but that there was zirconium. Moreover, the XRD analysis in Fig. 7(a) identified the precipitate as ZrO_2. The results of Run La-1 and La-2 were almost the same except for the amount of zirconium chloride remaining in the salt phase. One possible reason is that some oxygen impurity entered the Pyrex test tube for Run La-2 during the long stay in the furnace. The amount of lanthanum detected in the salt phase was about 82% of the calculated value based on the weight of La_2O_3 loaded. The discrepancy could be attributable to the La_2O_3 reagent that probably contained some moisture and $La(OH)_3$, which was examined in the Nd_2O_3 chlorination test described later.

When an insufficient amount of $ZrCl_4$ was loaded in Run La-3 and La-4, about 40% of the lanthanum dissolved and no $ZrCl_4$ remained in the salt. The precipitate of Run La-4 was in the form of fine particles as shown in Fig. 6(b). In the XRD pattern of Fig. 7(b), there are peaks for LaOCl and some broad peaks of unknown

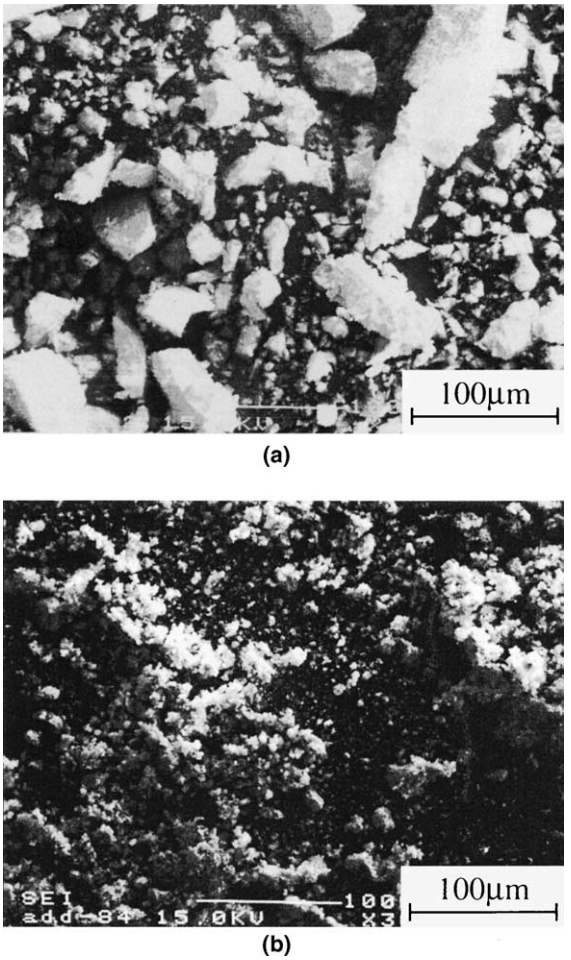

Fig. 6. Micrographs of precipitates obtained in the La_2O_3 chlorination test. (a) Run La-2, (b) Run La-4.

origin. They do not match the ZrO_2 peaks in Fig. 6(a) and might be attributable to La–Zr complex oxide. No peaks for La_2O_3 appeared in the XRD pattern. The results for Run La-3 and La-4 were almost the same.

The following can be concluded from the La_2O_3 chlorination tests. By adding $ZrCl_4$, La_2O_3 was first converted into LaOCl and simultaneously some La–Zr complex oxide might form. When an excess amount of $ZrCl_4$ was added, all of the lanthanum dissolved into the salt as trivalent ion and the ZrO_2 precipitated as a by-product. The reaction was completed within 8 h.

4.2.2. Nd_2O_3

Cyclic voltammograms (CVs) for $NdCl_3$ dissolved in a LiCl–KCl eutectic at 773 K were measured using a molybdenum working electrode. Typical CVs are shown in Fig. 8. There are two cathodic peaks. The large peak (A) at about −2.1 V vs. Ag/AgCl corresponds to the reduction of Nd(III) into neodymium metal. The small peak (B) at about −1.9 V is probably ascribable to the reduction of Nd(III) into Nd(II) [23,24]. The anodic peak (C) corresponds to the reoxidation of the deposited neodymium metal at the electrode surface. The CVs for the $ZrCl_4$–LiCl–KCl system have been described elsewhere [19]. The sharp cathodic peak for the reduction of Zr(IV) was observed at about −1.2 V.

In the Nd_2O_3 chlorination test, CVs were measured each time $ZrCl_4$ was added. Before the first $ZrCl_4$ addition, residual current was observed as shown in Fig. 9(a), which indicated that the Nd_2O_3 powder used in this test might contain some moisture and $Nd(OH)_3$. After the first $ZrCl_4$ addition, the residual current decreased due to the following reactions (Fig. 9(b)):

$$ZrCl_4 + 2H_2O \rightarrow ZrO_2 + 4HCl\uparrow \quad (5)$$

$$ZrCl_4 + 2OH^- \rightarrow ZrO_2 + 2Cl^- + 2HCl\uparrow \quad (6)$$

At the same time, some Nd_2O_3 was presumably converted into NdOCl. No current waves related to neodymium and zirconium were observed.

After the second $ZrCl_4$ addition, a pair of cathodic and anodic peaks ascribable to neodymium appeared (Fig. 9(c)). The height of the neodymium peak for Fig. 9(d)–(f) is the same, which indicated that all the Nd_2O_3 was chlorinated by the third $ZrCl_4$ addition. Therefore, the Zr(IV) reduction peak at about −1.2 V was increased by the last three $ZrCl_4$ additions. The change in the cathodic peak current at about −2.1 V was consistent with the analytical results of the salt samples. Fig. 10 exhibits the amount of neodymium and zirconium dissolved in the salt phase based on the ICP-AES analysis. There was a linear relationship between the cathodic peak current and the metal concentration in the salt for neodymium and zirconium.

The 0.224 g of Nd_2O_3 used in the test should contain 0.192 g of neodymium but finally only 0.140 g of neodymium was detected in the salt phase. To examine this discrepancy, the Nd_2O_3 reagent was dissolved in the nitric acid for the ICP-AES analysis. It was determined that the neodymium concentration was 81% of the expected value calculated from the weight of Nd_2O_3. Then, the Nd_2O_3 was examined by thermogravimetry. At about 593 K, a decrease in weight was observed, which indicated $Nd(OH)_3$ existed in the reagent.

The following can be concluded from the Nd_2O_3 test. All the Nd_2O_3 was chlorinated by adding an excess amount of $ZrCl_4$. By cyclic voltammetry, the approximate concentrations of neodymium and zirconium in the salt could be seen and so could the point at which the oxide was completely chlorinated.

4.2.3. Y_2O_3

A dense Y_2O_3 crucible was used as the oxide sample to be chlorinated. Fig. 11 shows the amount of zirconium

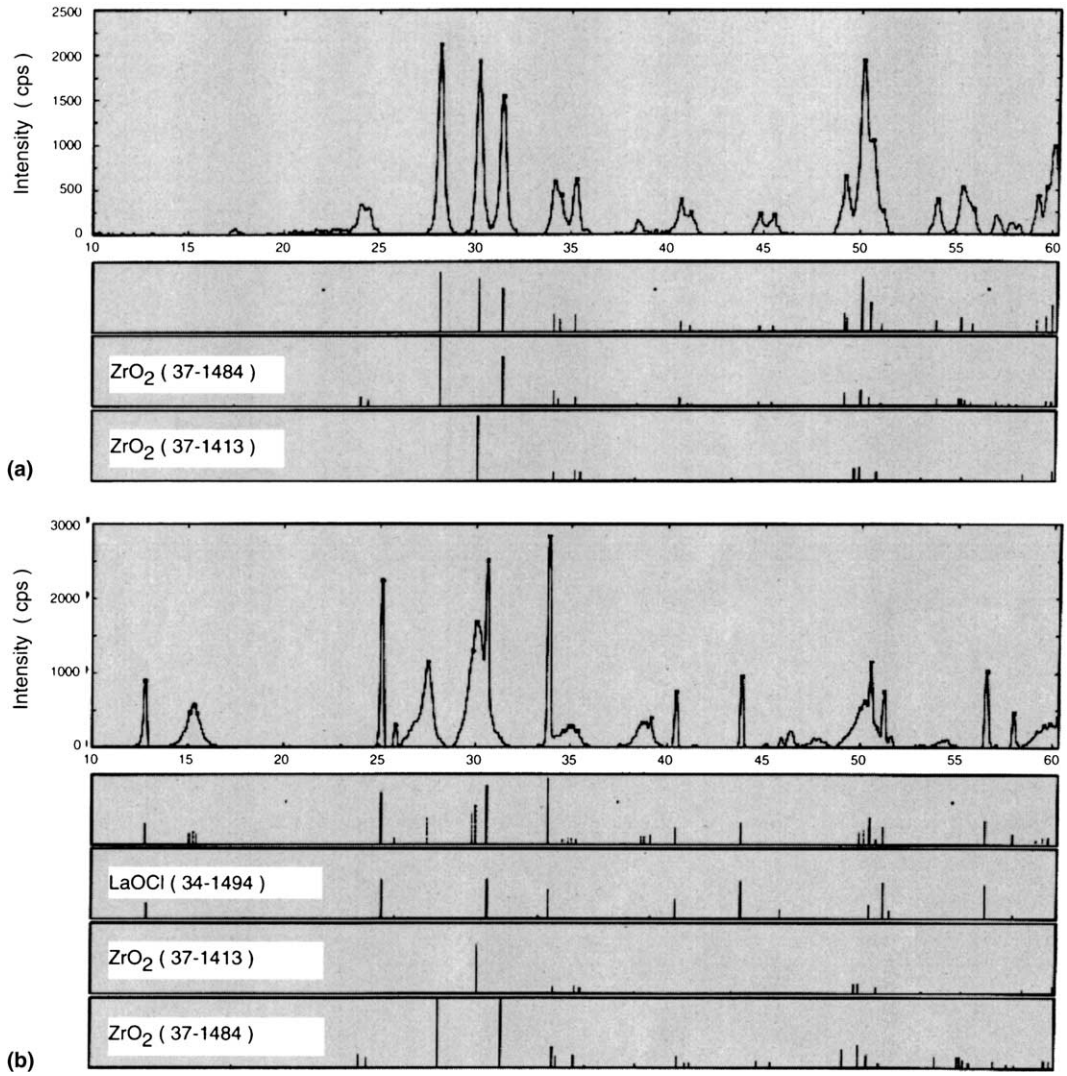

Fig. 7. X-ray diffraction pattern of precipitates obtained in the La_2O_3 chlorination test. (a) La-2, (b) La-4.

and yttrium dissolved in the salt phase after the $ZrCl_4$ addition. The zirconium concentration gradually decreased and the yttrium concentration increased. When 98 h had passed, about 89% of Y_2O_3 was dissolved and a small amount of $ZrCl_4$ remained in the salt. There were indications that even the sintered Y_2O_3 could be converted into chloride but it took a long time. Adding much more $ZrCl_4$, mixing the salt bath and crushing the sintered sample into powder would be effective in accelerating the reaction.

4.2.4. CeO_2

The results for Run Ce-1 using a zirconium metal reductant and Run Ce-2 using no reductant are shown in Fig. 12(a) and (b), respectively. The solid lines were drawn based on the mass balance calculation using the

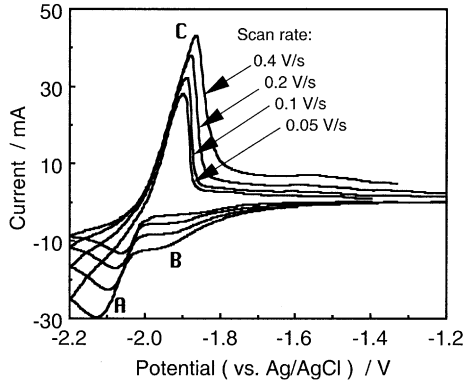

Fig. 8. Typical cyclic voltammograms for $NdCl_3$ in LiCl–KCl eutectic on a molybdenum electrode ($1\varnothing \times 10$ mm) at 773 K. Mole fraction of $NdCl_3$ in the salt, X_{NdCl_3}, was 0.0022.

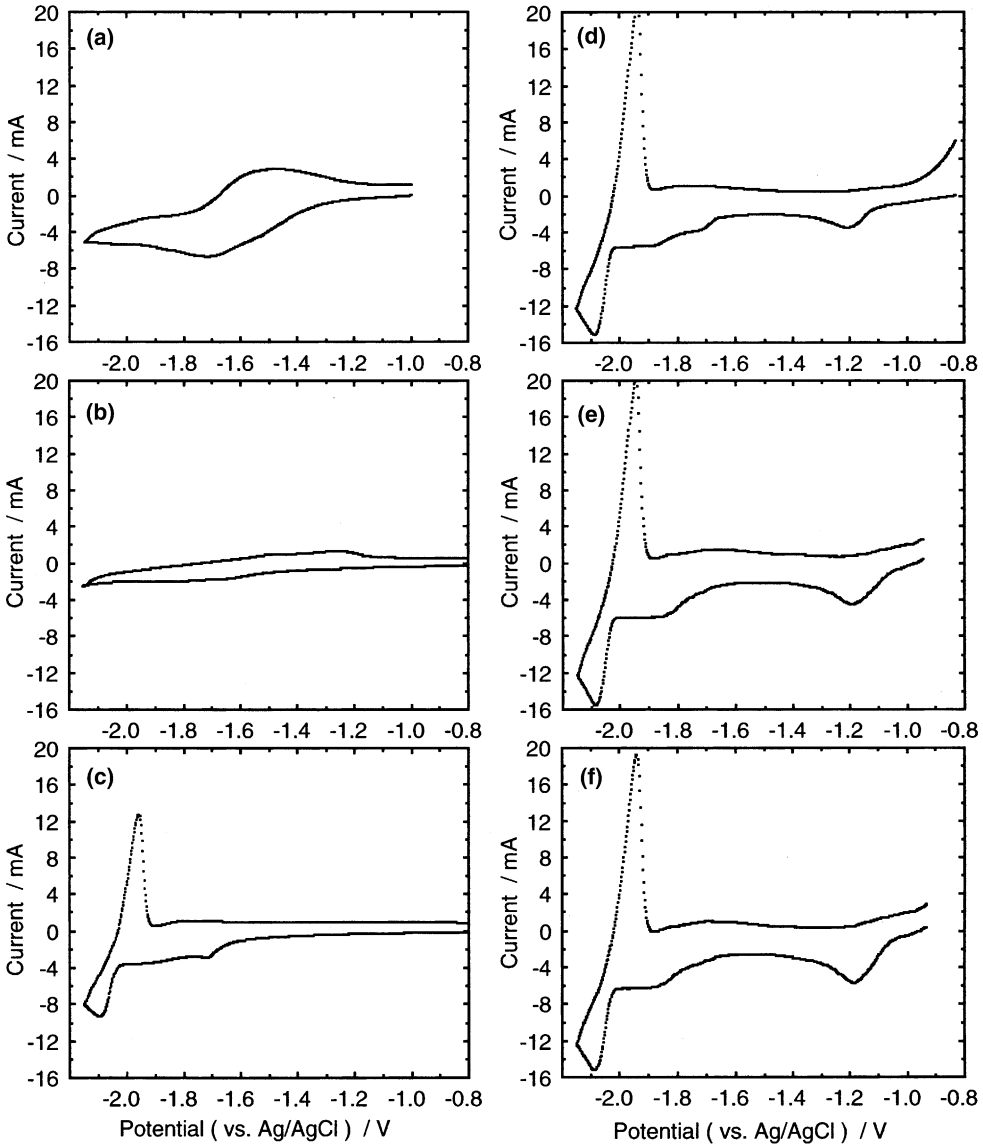

Fig. 9. Cyclic voltammograms during the Nd_2O_3 chlorination test. $ZrCl_4$ was added into the LiCl–KCl eutectic salt containing Nd_2O_3 five times: (a) before the $ZrCl_4$ additions; (b) after the first $ZrCl_4$ addition; (c) after the second $ZrCl_4$ addition; (d) after the third $ZrCl_4$ addition; (e) after the fourth $ZrCl_4$ addition; (f) after the fifth $ZrCl_4$ addition.

reaction (T14) in Table 1 for Run Ce-1 and the reaction (T15) for Run Ce-2. They are in good agreement with the values obtained by analyzing the salt samples.

It is obvious that all of the CeO_2 was chlorinated in both runs. In Run Ce-2, the CeO_2 might have been converted into chloride generating chlorine gas, which is to be expected from the value of ΔG° for the reaction (T15). In Run Ce-1, Zr(II) yielded by the reaction (2) would serve as a reductant:

$$CeO_2 + 1/2\,Zr(IV) + 1/2\,Zr(II) \rightarrow Ce(III) + ZrO_2 \qquad (7)$$

It was likely that chlorine gas was first yielded and then reacted with zirconium metal or Zr(II) to give Zr(IV). Therefore, the amount of $ZrCl_4$ needed for the chlorination in Run Ce-1 was 3/4 times as much as that in Run Ce-2 as shown in Fig. 12. Using zirconium metal reduced the consumption of $ZrCl_4$.

The $ZrCl_4$ addition was performed three times in both runs. The time dependence of the cerium concentration in the salt phase for Run Ce-1 is shown in Fig. 13. The $ZrCl_4$ concentration finally decreased below the detection limit of the ICP-AES when CeO_2 remained

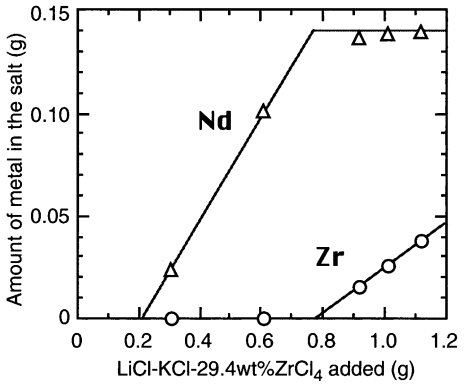

Fig. 10. The amounts of Nd and Zr dissolved in the salt as a function of the amount of LiCl–KCl-29.4wt%$ZrCl_4$ salt added.

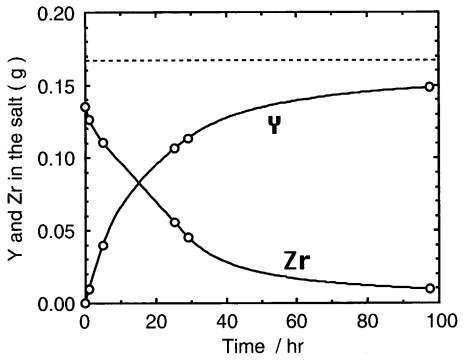

Fig. 11. Results of the Y_2O_3 test. The amount of Y and Zr dissolved in the salt after the $ZrCl_4$ addition. The dotted line indicates the amount of Y in the salt when the Y_2O_3 crucible is completely converted into chloride.

in the systems. It took several hours for the reaction to be completed for both runs.

4.3. Chlorination tests for actinide oxides

4.3.1. UO_2

The results of Run U-1 conducted in the presence of zirconium metal are shown in Fig. 14. The metal contents in the salt phase were plotted against the amount of $ZrCl_4$ added. Since the salt turned wine red, trivalent uranium appeared to be produced by the reaction. The solid lines were obtained by the mass balance calculation using the reaction (T1) in Table 1. The calculated results roughly agree with the analytical results. Zr(II) yielded by the reaction (2) might serve as a reductant and accelerate the chlorination.

$$UO_2 + 1/2\,Zr(IV) + 1/2\,Zr(II) \rightarrow U(III) + ZrO_2 \quad (8)$$

After the second $ZrCl_4$ addition, the time dependence of the metal chloride concentration in the salt phase was investigated as shown in Fig. 15. It is concluded that all of the UO_2 was chlorinated into U(III) within 3 h by adding an excess of $ZrCl_4$.

In Run U-2 conducted in the absence of zirconium metal, the Pyrex test tube was taken out from the furnace after 4 h. A UO_2 precipitate was observed at the bottom, and the salt turned yellow green, which indicated tetravalent uranium existed in the salt. The analysis of the salt sample determined that 37% of UO_2 was chlorinated and 79% of $ZrCl_4$ remained in the salt. As $UOCl_2$ is insoluble in molten chlorides [25], UCl_4 seemed to be yielded by the reaction (T2) shown in Table 1. $UOCl_2$ decomposes into UCl_4 and UO_2 as follows:

$$2\,UOCl_2 \rightarrow UCl_4 + UO_2 \quad (9)$$

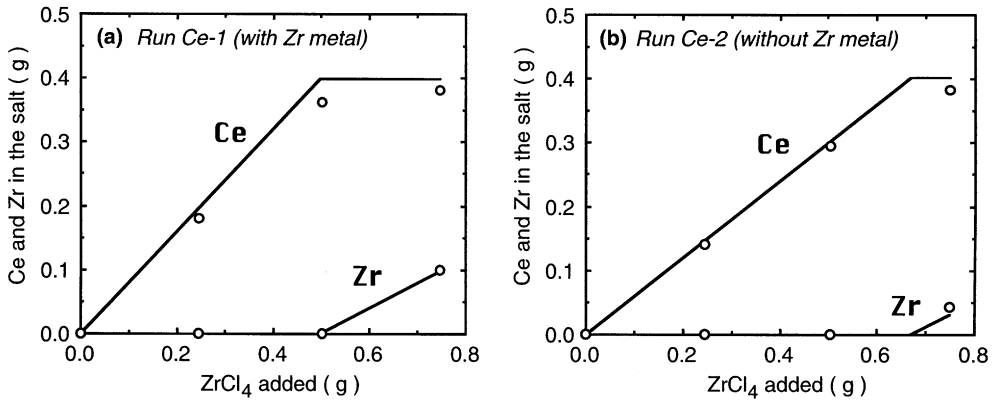

Fig. 12. The amount of Ce and Zr dissolved in the salt as a function of the amount of $ZrCl_4$ added. Solid lines were calculated using the following mass balance equations:

(a) $CeO_2 + 3/4\,ZrCl_4 + 1/4\,Zr \rightarrow CeCl_3 + ZrO_2$

(b) $CeO_2 + ZrCl_4 \rightarrow CeCl_3 + ZrO_2 + 1/2\,Cl_2$

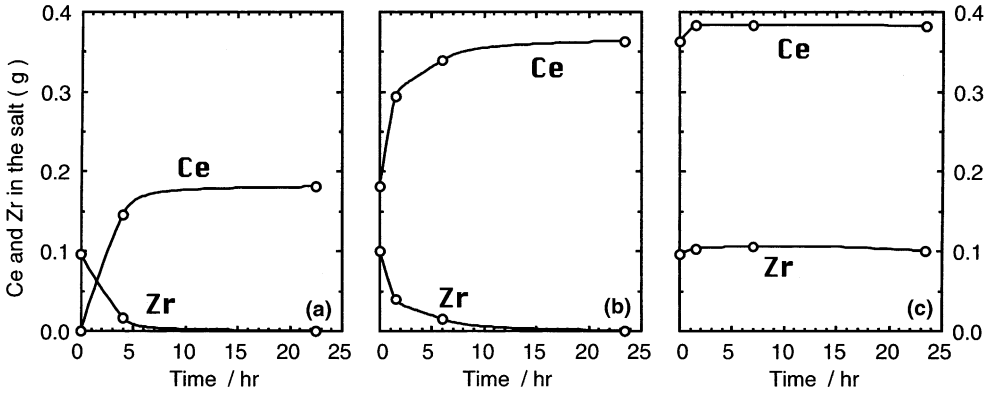

Fig. 13. Time dependence of the amount of Ce and Zr dissolved in the salt for Run Ce-1 after the (a) first, (b) second and (c) third $ZrCl_4$ addition.

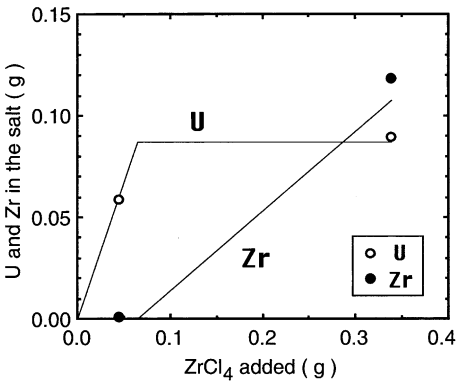

Fig. 14. Results for Run U-1. The amount of U and Zr dissolved in the salt as a function of the amount of $ZrCl_4$ added. The solid lines were calculated using the following mass balance equation:

$$UO_2 + 3/4\,ZrCl_4 + 1/4\,Zr \rightarrow UCl_3 + ZrO_2$$

ΔG° for the reaction (9) at 773 K is +7.6 kcal/mol-U according to the thermodynamic database [18]. Therefore, if the activity of UCl_4 in LiCl–KCl eutectic is less than $10^{-2.2}$, no $UOCl_2$ will exist in the system. At the end of the experiment, U(IV) concentration was 0.13 at.%, and the activity coefficient of tetravalent cation in the salt seems to be far less than unity because chloride ions coordinate around the cation. Hence, $UOCl_2$ might not have been produced in Run U-2.

UCl_4 is in equilibrium with $ZrCl_4$ as follows:

$$UO_2 + ZrCl_4 \rightleftarrows UCl_4 + ZrO_2 \qquad (10)$$

ΔG° for the reaction (10) is only −3.8 kcal/mol at 773 K [18]. Therefore, it is possible that $ZrCl_4$ and UCl_4 coexist in the salt, which will depend on their activity coefficients. Further studies are needed to determine the equilibrium constants and the activity coefficients.

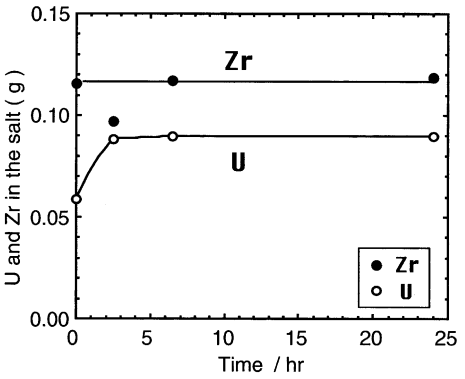

Fig. 15. Results for Run U-1. Time dependence of the amount of U and Zr dissolved in the salt after the second $ZrCl_4$ addition.

4.3.2. PuO_2

Since $PuCl_4$ is not stable compared with UCl_4, a reductant is necessary to chlorinate PuO_2. An excess amount of $ZrCl_4$ was initially loaded in the crucible and a zirconium metal wire was used for agitating the salt. Fig. 16 shows the time dependence of the amount of plutonium and zirconium dissolved in the salt. The dotted lines indicate the amount of metals that should exist in the salt phase when all of the PuO_2 was chlorinated by the reaction (T8) as shown in Table 1. It is obvious that the PuO_2 was completely chlorinated within 3.5 h. It appears that chlorination of PuO_2 can be achieved easily.

The results of the chlorination tests for rare earth and actinide oxides are summarized in Table 6.

5. Conclusion

$ZrCl_4$, which sublimes above 573 K, has a high reactivity with oxygen. Once $ZrCl_4$ dissolves into LiCl–KCl

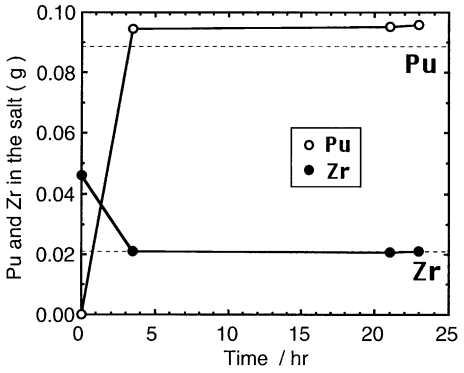

Fig. 16. The amount of Pu and Zr dissolved in the salt after the salt melted in the furnace at 773 K. The dotted lines are the calculated values based on the following mass balance equation:

$$PuO_2 + 3/4\,ZrCl_4 + 1/4\,Zr \rightarrow PuCl_3 + ZrO_2$$

eutectic salt, $ZrCl_4$ does not vaporize. The solubility of $ZrCl_4$ in the salt was measured to be 0.013 at.% at 773 K. Rare earth oxides (La_2O_3, CeO_2, Nd_2O_3 and Y_2O_3) and actinide oxides (UO_2 and PuO_2) were allowed to react with $ZrCl_4$ in the salt bath at 773 K to give a metal chloride solution and a precipitate of ZrO_2. The thermodynamic estimation suggested that UO_2 should be the most difficult oxide to chlorinate in this group. Zirconium metal was used as a reductant when dioxides were chlorinated. Zr(II), which is yielded by the disproportionation reaction of zirconium metal and Zr(IV), might accelerate the chlorination of the dioxides. As a result, all of the oxides were chlorinated and dissolved into the salt as trivalent species by adding an excess of $ZrCl_4$. The oxides in powder form were mostly chlorinated within 5 h. When no reductant was used, UO_2 and CeO_2 were converted into U(IV) and Ce(III), respectively. Electrochemical measurements such as cyclic voltammetry proved useful to determine when the reaction was completed. The by-product of ZrO_2 was fine white powder. When the system was kept still, the solution settled so that the ZrO_2 precipitate could be separated.

It was experimentally demonstrated that UO_2, PuO_2 and rare earth oxides were completely chlorinated using $ZrCl_4$ in a molten salt bath. Thermodynamic considerations indicate that the minor actinide oxides will also be chlorinated. This chlorination method has the following advantages:

- Very simple.
- The reaction rate is sufficient.
- $ZrCl_4$ is not corrosive to refractory metals such as steel.
- Flexibility for scale, molten salt composition and temperature.
- Actinide metals as well as oxides are chlorinated.
- The by-product of ZrO_2 is quite stable.

This method is quite compatible with the electrorefining process for the metal fuel cycle shown in Fig. 1 because zirconium is a major component of the metal fuel and LiCl–KCl eutectic salt is used as the salt bath. From the point of view of waste reduction, it is possible that $ZrCl_4$ is produced from the cladding hulls of the light water reactor fuel. Examples of the application to the pyrometallurgical process are as follows:

1. Actinide chlorides have to be periodically supplied for the electrorefiner. UCl_3 and $PuCl_3$ can be produced from UO_2 and PuO_2 by this method.
2. Actinide dissolved in a molten chloride precipitates as oxide or oxychloride when oxygen impurities are carried into the salt. By adding $ZrCl_4$, the actinide precipitates can be dissolved into the salt again. Therefore, a high recovery ratio for actinides can be attained.

Table 6
Summary of the chlorination tests for rare earth and actinide oxides

Oxide (run no.)	Total weight (g)		Reductant	Reaction time (h)	% metal detected in the salt phase	Observations
	Oxide	$ZrCl_4$				
La_2O_3 (La-1)	0.196	0.236	Not used	8	82[a]	Completely chlorinated
Nd_2O_3	0.224	0.330	Not used	72	73[a]	Completely chlorinated
Y_2O_3[b]	0.212	0.345	Not used	98	89	Y_2O_3 remained
CeO_2 (Ce-1)	0.490	0.747	Zr metal	55	96	Completely chlorinated
CeO_2 (Ce-2)	0.494	0.749	Not used	55	95	Completely chlorinated
UO_2 (U-1)	0.099	0.339	Zr metal	24	103	Completely chlorinated
UO_2 (U-2)	0.190	0.157	Not used	4	37	UO_2 remained
PuO_2	0.101	0.117	Zr metal	3.5	107	Completely chlorinated

[a] The La_2O_3 and Nd_2O_3 reagents contained H_2O and hydroxide.
[b] A sintered Y_2O_3 crucible was used. The oxides except for Y_2O_3 were in powder form.

3. During the injection casting operation for manufacturing the U–Pu–Zr fuel slugs [12,13], part of actinide metals may react with crucible coating materials or oxygen impurities to give some dross consisting of UO_2 and PuO_2. The actinides in the dross can be easily recycled in the electrorefiner by this chlorination method. In addition, the actinide metals attaching to the dross are also chlorinated according to the standard potential data of zirconium and actinides in the LiCl–KCl eutectic system [26,27].
4. Actinide oxides and metals may adhere to wastes such as the cladding hull and crucible. The wastes can be decontaminated by washing with a molten salt containing $ZrCl_4$.
5. Actinides in spent oxide fuels can be chlorinated and dissolved into a molten salt, followed by the electrorefining process to collect the actinides.

The efficient separation of the ZrO_2 precipitate from the molten salt is a problem that will need to be resolved in the future. For that purpose, centrifuges may prove to be useful.

Acknowledgments

The authors are grateful to Dr M. Kurata and Mr M. Iizuka of CRIEPI for their helpful suggestions. We wish to thank Dr Y. Arai of JAERI for his support and useful advice with the plutonium experiment. We appreciate the assistance provided by the staff of Kyoto University Research Reactor Institute where the uranium tests were performed.

References

[1] Y.I. Chang, Nucl. Technol. 88 (1989) 129.
[2] J.J. Laidler, J.E. Battles, W.E. Miller, E.C. Gay, in: Proceedings of Future Nuclear Systems: Emerging Fuel Cycles and Waste Disposal Options, Global'93, vol. 2, Seattle, WA, 12–17 September 1993, p. 1061.
[3] T. Inoue, T. Yokoo, T. Nishimura, in: Proceedings of International Conference on Future Nuclear Systems, GLOBAL'99, Jackson Hole, WY, 29 August–3 September 1999.
[4] S.X. Li, in: Proceedings of 8th International Conference on Nuclear Engineering (ICONE-8), Baltimore, MD, 2–6 April 2000.
[5] K. Kinoshita, T. Koyama, T. Inoue, M. Ougier, J.-P. Glatz, J. Phys. Chem. Solid, in press.
[6] Z. Tomczuk, J.P. Ackerman, R.D. Wolson, W.E. Miller, J. Electrochem. Soc. 139 (12) (1992) 3523.
[7] T.C. Totemeier, R.D. Mariani, J. Nucl. Mater. 250 (1997) 131.
[8] T. Koyama, M. Iizuka, Y. Shoji, R. Fujita, H. Tanaka, T. Kobayashi, M. Tokiwai, J. Nucl. Sci. Technol. 34 (4) (1997) 384.
[9] M. Iizuka, K. Uozumi, T. Inoue, T. Iwai, O. Shirai, Y. Arai, J. Nucl. Mater. 299 (2001) 32.
[10] K. Uozumi, M. Iizuka, T. Kato, T. Inoue, O. Shirai, T. Iwai, Y. Arai, J. Nucl. Mater. 325 (2004) 34.
[11] B.R. Westphal, D. Vaden, T.Q. Hua, J.L. Willet, D.V. Laug, in: Proceedings of 5th Topical Meeting, DOE Owned Spent Nuclear Fuel and Fissile Materials Management, Charleston, SC, 17–20 September 2002.
[12] D.B. Tracy, S.P. Henslee, N.E. Dodds, K.J. Longua, Trans. Am. Nucl. Soc. 60 (1989) 314.
[13] M. Tokiwai, A. Kondo, R. Yuda, N. Tsukino, S. Yoshie, M. Izaki, T. Izumiya, T. Furuya, in: Proceedings of Actinide 2001 International Conference, Hayama, Japan, 4–9 November 2001, J. Nucl. Sci. Technol. (Suppl. 3) (2002) 910.
[14] E.J. Karell, R.D. Pierce, T.P. Mulcahey, in: Proceedings of DOE Spent Nuclear Fuel and Fissile Material Management, Reno, NV, 16–20 June 1996, p. 352.
[15] T. Usami, M. Kurata, T. Inoue, H.E. Sims, S.A. Beetham, J.A. Jenkins, J. Nucl. Mater. 300 (2002) 15.
[16] T. Usami, T. Kato, M. Kurata, T. Inoue, H.E. Sims, S.A. Beetham, J.A. Jenkins, J. Nucl. Mater. 304 (2002) 50.
[17] M. Kurata, K. Kinoshita, T. Hijikata, T. Inoue, J. Nucl. Sci. Technol. 37 (8) (2000) 682.
[18] Japan Calorimetry Society, Thermodynamic Data Base MALT-II, Kagaku-gijutsusya, 1992.
[19] Y. Sakamura, J. Electrochem. Soc. 151 (3) (2004) C187.
[20] R.D. Shannon, Acta Cryst. A 32 (1976) 751.
[21] J. Kipouros, J.H. Frint, D.R. Sadoway, Inorg. Chem. 24 (1985) 3881.
[22] G.J. Kipouros, S.N. Flengas, J. Electrochem. Soc. 132 (5) (1985) 1087.
[23] Y. Sakamura, H. Miyashiro, T. Matsumoto, CRIEPI Report, T91003, 1991 (in Japanese).
[24] I. Wu, H. Zhu, Y. Sato, T. Yamamura, K. Sugimoto, in: Proceedings of 9th International Symposium on Molten Salts, Electrochemical Society, vol. 94-13, 1994, p. 504.
[25] R. Kein, C. Keller (Eds.), Gmelin Handbook of Inorganic Chemistry, U Suppl. vol. C5, Springer-Verlag, Berlin, 1986, p. 295.
[26] Y. Sakamura, T. Hijikata, K. Kinoshita, T. Inoue, T.S. Storvick, C.L. Krueger, J.J. Roy, D.L. Grimmett, S.P. Fusselman, R.L. Gay, J. Alloys Comp. 271–273 (1998) 592.
[27] J.A. Plambeck, in: A.J. Bard (Ed.), Fused Salt Systems, Encyclopedia of Electrochemistry of the Elements, vol. X, Marcel Dekker, NY, Basel, 1976.